

Contribution for the JETP special issue in honor of L.V. Keldysh's 85th birthday

Electron–Positron Pair Production from Vacuum in the Field of High-Intensity Laser Radiation

V. S. Popov^a, V. D. Mur^b, N. B. Narozhnyi^b, and S. V. Popruzhenko^{b*}

^a Institute of Theoretical and Experimental Physics, ul. Bol'shaya Cheremushkinskaya 25, Moscow, 117218 Russia

^b National Research Nuclear University MEPhI, Kashirskoe sh. 31, Moscow, 115409 Russia

*e-mail: sergey.popruzhenko@gmail.com

Received August 5, 2015

Abstract—The works dealing with the theory of e^+e^- pair production from vacuum under the action of high-intensity laser radiation are reviewed. The following problems are discussed: pair production in a constant electric field \mathcal{E} and time-variable homogeneous field $\mathcal{E}(t)$; the dependence of the number of produced pairs $N_{e^+e^-}$ on the shape of a laser pulse (dynamic Schwinger effect); and a realistic three-dimensional model of a focused laser pulse, which is based on exact solution of Maxwell's equations and contains parameters such as focal spot radius R , diffraction length L , focusing parameter Δ , pulse duration τ , and pulse shape. This model is used to calculate $N_{e^+e^-}$ for both a single laser pulse ($n = 1$) and several ($n \geq 2$) coherent pulses with a fixed total energy that simultaneously “collide” in a laser focus. It is shown that, at $n \gg 1$, the number of pairs increases by several orders of magnitude as compared to the case of a single pulse. The screening of a laser field by the vapors that are generated in vacuum, its “depletion,” and the limiting fields to be achieved in laser experiments are considered. The relation between pair production, the problem of a quantum frequency-variable oscillator, and the theory of groups $SU(1, 1)$ and $SU(2)$ is discussed. The relativistic version of the imaginary time method is used in calculations. In terms of this version, a relativistic theory of tunneling is developed and the Keldysh theory is generalized to the case of ionization of relativistic bound systems, namely, atoms and ions. The ionization rate of a hydrogen-like ion with a charge $1 \leq Z \leq 92$ is calculated as a function of laser radiation intensity \mathcal{I} and ellipticity ρ .

DOI: 10.1134/S1063776116030171

1. INTRODUCTION

The basic relativistic quantum mechanics equation—the Dirac equation—was discovered in 1928 [1, 2] and was applied by Gordon [3] and Darwin [4] in that year to explain the fine structure of a hydrogen-like atom [5]. Three years later, Sauter [6] discussed the production of e^+e^- pairs from vacuum in an electric field in relation to the so-called Klein paradox (see, e.g., [7]). In the presence of a constant and homogeneous field \mathcal{E} , the probability of vacuum–vacuum transition differs from unity: Heisenberg and Euler were the first to calculate it in a principal approximation [8], and exact formulas were derived by Schwinger [9] for particles with spin $s = 0$ and $s = 1/2$ and by Vanyashin and Terent'ev [10] for the case of vector bosons at $s = 1$ (also see [11]).

Until recently, the pair production in a strong field was considered to be of only theoretical interest, since its detection needs the electric fields that are comparable with the “critical” field of quantum electrodynamics [8] (see Eq. (1) below), which is higher than the

experimentally achievable fields by many orders of magnitude. Nevertheless, rapid progress in laser physics and engineering led to a substantial increase in available laser radiation intensity \mathcal{I} . Ultrahigh fields can be reached upon the compression (shortening) of laser pulses, the duration of which τ becomes comparable with the optical period ($\tau \sim 10^{-15}$ s for femtosecond pulses from the infrared wavelength range) and the shape of which is far from an ideal sinusoid.

Ultrahigh-intensity pulses are generated using solid-state lasers with near-infrared and optical wavelengths: neodymium (wavelength $\lambda = 1064$ nm) and titanium–sapphire ($\lambda \approx 800$ nm) lasers and their second harmonics are most widely used. Modern laser facilities can generate pulses with an intensity up to $\mathcal{I} \approx 2 \times 10^{22}$ W/cm² (electric field strength in this case ($\mathcal{E}_0 \approx 10^{12}$ V/cm) is higher than the atomic field strength by 2–3 orders of magnitude, and the duration of pulses of such an intensity is several tens of femtoseconds) [12]. The appearance of powerful free electron lasers (FELs) opened up fresh opportunities for

experiments on nonlinear interaction of laser radiation with a substance in the ultraviolet and X-ray wavelength ranges. Such laser are used in Germany [13], Japan [14], and the United States [15, 16]. The record laser pulse intensities achieved in FELs are 10^{16} W/cm² at a wavelength $\lambda \approx 13$ nm (DESY laboratory, Germany), 10^{14} W/cm² at $\lambda \approx 50$ nm (SPRING-8 laser, Japan), and 10^{18} W/cm² at $\lambda \approx 1.2$ nm (SLAC-based FEL, United States). The nonlinear character of interaction of powerful electromagnetic radiation with a substance manifests itself at much lower intensities.

The modern technically grounded projects of creating new lasers [17–20] suggest an increase in the maximum achievable intensity by several orders of magnitude, up to 10^{25} – 10^{26} W/cm² [20–23]. New experimental possibilities quickened interest in theoretical investigations of particle production from vacuum in an intense electromagnetic field (e.g., see [22–26] and references cited therein). This fact justifies the appearance of this article, which continues review [27] and mainly covers our works.

In conclusion of this section, we present the intensities and electromagnetic fields that characterize vapor production from vacuum and the nonlinear ionization of atomic systems and some other quantities to be used in this work. Here, we use the designations from [27–33]. The critical field of quantum electrodynamics [8] and the corresponding intensity of a linearly polarized plane wave are

$$\begin{aligned} \mathcal{E}_{\text{cr}} &= m^2 c^3 / e \hbar = 1.32 \times 10^{16} \text{ W/cm}, \\ \mathcal{I}_{\text{cr}} &= c \mathcal{E}_{\text{cr}}^2 / 8\pi \approx 2.3 \times 10^{29} \text{ W/cm}^2, \end{aligned} \quad (1)$$

where m is the electron mass, e is the elementary charge, and c is the velocity of light. The critical field is determined from the condition $e \mathcal{E}_{\text{cr}} l_C = mc^2$, where

$$l_C = \hbar / mc = 3.86 \times 10^{-11} \text{ cm} \quad (2)$$

is the Compton wavelength. The atomic field and the corresponding intensity are expressed as

$$\begin{aligned} \mathcal{E}_a &= m^2 e^5 / \hbar^4 = \alpha^3 \mathcal{E}_{\text{cr}} \approx 5.1 \times 10^9 \text{ W/cm}, \\ \mathcal{I}_a &= c \mathcal{E}_a^2 / 8\pi \approx 3.5 \times 10^{16} \text{ W/cm}^2, \end{aligned} \quad (3)$$

where $\alpha = e^2 / \hbar c \approx 1/137$ is the fine structure constant.

2. IMAGINARY TIME METHOD IN RELATIVISTIC QUANTUM MECHANICS

An analytical description of the ionization of atoms, ions, and solids under high-intensity laser radiation is based on fundamental work by Keldysh [34], the 50th anniversary of which caused review [27] and special issue of Journal of Physics B [35]. The approach proposed in that work led to the development of several effective methods of an analytical calculation of the probabilities of the nonlinear quantum effects induced a strong electromagnetic field, such as

the ionization of atoms and ions, the generation of laser radiation harmonics, and electron–positron pair production by a laser field from vacuum.

At present, the imaginary time method (ITM) is widely used in the physics of strong laser fields. This method was likely to be developed for the first time in the theory of multiphoton atom ionization by high-intensity laser light [36–38]. It is the generalization of the well-known method of complex classical Landau trajectories to the case of time-variable fields (see [39; 40, Sections 51, 52]). Examples of using ITM in quantum mechanics and the field theory, including the problem of e^+e^- pair production by laser radiation from vacuum, are given in [28, 29, 41, 42]. This method and its applications were described in detail in reviews [27, 31, 43]. In particular, in [27] we discussed the use of the imaginary proper time method (Fock method) to solve the problem of vapor production from vacuum by constant and homogeneous mutually perpendicular electric and magnetic fields. ITM uses classical equations of motion but with imaginary “time” ($t \rightarrow it$), and their solutions make it possible to determine the subbarrier particle (electron) trajectory along which tunneling occurs. Taking into account the Feynman relation $\Psi \propto \exp(iS/\hbar)$, where S is the classical action accumulated by a particle moving along a subbarrier trajectory, an calculating $\text{Im}S$, we find the probability of tunneling (in this case, the ionization of an atomic level or pair production from vacuum by a strong laser field).

Due to the development of laser physics and technology in recent years, intensities [12] of about $\mathcal{I} \approx 2 \times 10^{22}$ W/cm² were reached and they are going to be increased by several orders of magnitude. The electron motion (including subbarrier motion) in such strong fields becomes relativistic, which calls for a modification of ITM and the Keldysh theory of ionization. These problems were considered and some results are presented below (we mainly follow works [42, 43]).

2.1. Relativistic Theory of Tunneling

We now consider the application of ITM to the problem of the ionization of the relativistic bound state of a hydrogen-like ion. In the case of a monochromatic wave with frequency ω and ellipticity ρ moving in vacuum along axis x , we have

$$\begin{aligned} \mathcal{E}_x &= \mathcal{H}_x = 0, & \mathcal{E}_y &= \mathcal{E}_0 \cos \theta, & \mathcal{E}_z &= \rho \mathcal{E}_0 \sin \theta, \\ \mathcal{H}_y &= -\rho \mathcal{E}_0 \sin \theta, & \mathcal{H}_z &= \mathcal{E}_0 \cos \theta, \\ \theta &= \omega(t - x), & -1 &\leq \rho \leq 1, \end{aligned} \quad (4)$$

where \mathcal{E}_0 is the wave amplitude and θ is the variable of the light front ($\hbar = c = 1$).

Table 1. Ionization rate w_r for the $1s_{1/2}$ level of a hydrogen-like atom with charge Z

$\log \mathcal{F}$	$F \cdot 100$	w_r	$\log \mathcal{F}$	$F \cdot 100$	w_r
$Z = 20, \epsilon_0 = 0.989, \mathcal{E}_{\text{ch}} = 4.13(13)$			$Z = 40, \epsilon_0 = 0.956, \mathcal{E}_{\text{ch}} = 3.38(14)$		
20.5	1.18	1.5(-4)	22.0	0.81	—
21.0	2.10	6.4(6)	22.5	1.44	12
21.5	3.73	5.4(12)	23.0	2.56	6.2(9)
22.0	6.63	1.0(16)	23.5	4.55	4.3(14)
22.5	11.8	6.4(17)	24.0	8.09	2.1(17)
$Z = 60, \epsilon_0 = 0.899, \mathcal{E}_{\text{ch}} = 1.19(15)$			$Z = 92, \epsilon_0 = 0.741, \mathcal{E}_{\text{ch}} = 4.82(15)$		
23.5	1.30	0.120	24.5	1.01	4.7(-8)
24.0	2.30	6.0(8)	25.0	1.80	1.6(5)
24.5	4.10	1.6(14)	25.5	3.20	1.8(12)
25.0	7.29	1.6(17)	26.0	5.68	1.7(16)
25.5	9.72	6.5(18)	26.5	10.1	2.9(18)

The application of ITM gives the subbarrier trajectory that relates the initial state of electron in a discrete spectrum to its final state in continuum in the form

$$\begin{aligned}
 x &= -i \frac{e^2 \mathcal{E}_0^2}{J^2 \omega^2} \left\{ \frac{1}{8} (1 - \rho^2) \left[\sinh 2\eta - \eta \frac{\sinh 2\eta_0}{\eta_0} \right] \right. \\
 &\quad \left. + \rho^2 \left(\frac{\sinh \eta_0}{\eta_0} \left[\sinh \eta - \eta \frac{\sinh \eta_0}{\eta_0} \right] \right) \right\}, \\
 y &= \frac{e \mathcal{E}_0}{J \omega^2} (\cosh \eta_0 - \cosh \eta), \\
 z &= -i \rho \frac{e \mathcal{E}_0}{J \omega^2} \left[\sinh \eta - \eta \frac{\sinh \eta_0}{\eta_0} \right], \quad t = x(\eta) + i \omega^{-1} \eta,
 \end{aligned} \tag{5}$$

where $\eta = -i\theta$ and

$$J = (\sqrt{p^2 + m^2} - p_x)/m \tag{6}$$

is the integral of motion [44]. As is seen from Eq. (5), variables x and z (and p_y) are purely imaginary under a barrier; therefore, such a trajectory is impossible in classical mechanics. However, it is this trajectory that determines the tunneling probability, i.e., rate w of atom ionization by laser radiation, in quantum mechanics.

The calculation of the truncated action function [43, 45] along trajectory (5),

$$\text{Im } W = \text{Im} \int_{t_0}^0 \{-\sqrt{1 - \mathbf{v}^2} + e \mathbf{A} \mathbf{v} + \epsilon_0\} dt, \tag{7}$$

where \mathbf{A} is the vector potential of field (4), \mathbf{v} is the electron velocity, $m\epsilon_0 \equiv E_0 = m\sqrt{1 - (Z\alpha)^2}$ is the initial energy of the level, yields the probability of ionization of relativistic level s

$$w_r \propto \exp\{-2 \text{Im } W\} = \exp\left\{-\frac{2m}{\omega} \eta_0 (J - \epsilon_0)\right\} \tag{8}$$

provided that $\omega \ll m$. The values of parameters η_0 and J that correspond to the time when an electron leaves the barrier can be found from the boundary conditions of ITM and are determined by the equations presented in [42]. As a result, we obtain

$$w_r \propto \exp\left\{-\frac{2}{3F} g(\gamma_R, \epsilon, \rho)\right\}, \tag{9}$$

where $F = \mathcal{E}/\mathcal{E}_{\text{ch}}$ is the reduced field; \mathcal{E}_{ch} is the characteristic field,

$$\begin{aligned}
 \mathcal{E}_{\text{ch}} &= (\sqrt{3}\xi)^3 (1 + \xi^2)^{-1} \mathcal{E}_{\text{cr}} \\
 &= \begin{cases} Z^3 \mathcal{E}_a, & Z \ll 137, \\ 2.60 \mathcal{E}_{\text{cr}}, & Z = 137, \end{cases}
 \end{aligned} \tag{10}$$

which is close to the electric field in the K th shell of a hydrogen-like atom (ion) with charge Z ; γ_R is the relativistic analog of the Keldysh adiabaticity parameter,

$$\gamma_R = \frac{m\omega}{e\mathcal{E}_0} \sqrt{\frac{3\xi^2}{1 + \xi^2}} \equiv \frac{\gamma_r}{\sqrt{1 - \xi^3/3}}, \tag{11}$$

ξ is convenient auxiliary variable that naturally appears in ITM,

$$\begin{aligned}
 \xi(\epsilon) &= \left[1 - \frac{1}{2} \epsilon (\sqrt{\epsilon^2 + 8} - \epsilon) \right]^{1/2} \\
 &= \begin{cases} 3^{-1/2} \alpha \kappa, & \epsilon = 1 - \frac{1}{2} \alpha^2 \kappa^2 \rightarrow 1, \\ 1 - 2^{-1/2} \epsilon, & \epsilon \rightarrow 0, \end{cases}
 \end{aligned} \tag{12}$$

and $\kappa = \sqrt{-2\epsilon_0}$. The physical meaning of parameters γ_R and γ_r and the relation between them are discussed in Appendix B. The atoms known to date have $Z < 137$ and $1 > \epsilon > 0$, or $0 < \xi < 1$, and the point nuclear charge approximation can be used in this case. For-

mula (9) determines the ionization rate of the relativistic s th level to an accuracy of a preexponential factor at any values of ϵ and ρ .

For optical and infrared lasers, we have $\hbar\omega/mc^2 \approx 10^{-5}$; therefore, function g in Eq. (9) can be expanded into a series in parameter $\gamma_r \ll 1$,

$$w_r \propto \exp \left\{ -\frac{2\kappa^3}{3\epsilon_0} \left[1 - \frac{1-\rho^2/3}{10(1-\xi^2/3)} \gamma_r^2 + \mathcal{O}(\gamma_r^4) \right] \right\}. \quad (13)$$

Equations (9)–(13) yield a relativistic generalization of the Keldysh theory of ionization. The preexponential and Coulomb factors were calculated in [46, 47]. In the nonrelativistic limit, we have $\epsilon_0 = \sqrt{1-(Z\alpha)^2} \rightarrow 1$, $\xi \rightarrow 0$, and $\gamma_r \rightarrow \gamma$ (where γ is the Keldysh parameter [27, 34]). Equation (13) coincides with the results obtained in [36, 37, 48] for the case of linear ($\rho = 0$) or circular ($\rho = \pm 1$) polarization. In conclusion, we present the results of the numerical calculations performed using a model of a hydrogen-like atom (ion) with charge $Z < 137$.

As is seen from the values given in Table 1, the dependence of the ionization rate on intensity \mathcal{I} and charge Z is an extremely sharp function of the laser radiation intensity: when the intensity increases by two orders of magnitude, the ionization probability increases by 20–25 orders of magnitude; when the nuclear charge increases from 20 to 40 at a fixed intensity, this probability decreases by more than 16 orders of magnitude.

2.2. Constant and Low-Frequency Fields

ITM can be used to solve the problem of ionization of the s th level bound by short-range forces in constant and homogeneous fields \mathcal{E} and \mathcal{H} . In the nonrelativistic limit, we have $\epsilon_0 = 1 - \alpha^2\kappa^2/2 \rightarrow 1$ and $\kappa = \sqrt{-2\epsilon_0} \approx 1$; the following well-known formulas for the ionization rate of negative ions (H^- , Na^- , etc.) are obtained in this case [49]:

$$w_0 = \frac{|A_\kappa|^2}{2} \kappa^2 F \exp\left(-\frac{2}{3F}\right), \quad F = \frac{\mathcal{E}}{\kappa^3}, \quad (14)$$

where A_κ is the asymptotic (for $r \rightarrow \infty$) coefficient of the wavefunction of the bound state in zero field.

In the case of mutually perpendicular fields $\mathcal{E} \perp \mathcal{H}$, we obtain [48]

$$w_0 = \frac{1}{2} |A_\kappa|^2 \kappa^2 F \times \exp \left\{ -\frac{2}{3F} \left[1 + \frac{\alpha^2 \kappa^2}{30 \epsilon_0^2} \left(\mathcal{H}^2 - \frac{9}{4} \mathcal{E}^2 \right) \right] \right\}, \quad (15)$$

which gives the ionization probability of negative ions with allowance for corrections on the order of α^2 . Finally, in the limit $\epsilon_0 \rightarrow 1$ (i.e., when binding energy

E_0 approaches the boundary of lower continuum), we obtain [46]

$$w_0(\mathcal{E}, \mathcal{H}) = 2 \text{Im} S = \frac{\alpha}{2\pi} \frac{\mathcal{E} \mathcal{H}}{\sinh(\pi \mathcal{H}/\mathcal{E})} \exp\left(-\frac{\pi \mathcal{E}_a}{\mathcal{E}}\right), \quad (16)$$

which agrees with the first term of the Schwinger expansion for the imaginary part of the effective action function in scalar electrodynamics [9]. In particular, at $\mathcal{H} = 0$, Eq. (16) gives the probability of e^+e^- pair production from vacuum in constant electric field \mathcal{E} ,

$$w_0(\mathcal{E}) = \frac{m^4}{2\pi^2} \left(\frac{\mathcal{E}}{\mathcal{E}_{\text{cr}}} \right)^2 \exp\left(-\frac{\pi \mathcal{E}_{\text{cr}}}{\mathcal{E}}\right), \quad (17)$$

$\mathcal{E} \ll \mathcal{E}_{\text{cr}}$,

where $m^{-4} = l_c^3 \tau_c = 7.35 \times 10^{-53} \text{ cm}^3 \text{ s}$ is the relativistically invariant 4-volume and $\tau_c = l_c/c = 1.3 \times 10^{-21} \text{ s}$.

In the problem of electron motion in a constant or low-frequency crossed field ($\mathcal{E} = \mathcal{H}$, $\mathcal{E} \perp \mathcal{H}$, $\omega \ll \kappa^2$), an extremum subbarrier trajectory is analytically determined.¹ At the initial time $t = t_0$ of subbarrier motion, “time” is purely imaginary,

$$t_0 = i \sqrt{\frac{3\xi^2}{1+\xi^2}} \frac{\mathcal{E}_{\text{cr}}}{\mathcal{E}}, \quad (18)$$

and $\mathbf{r}(t_0) = 0$ according to the fact that the electron is inside an atom. At the exit from the barrier ($t = 0$), we have

$$r(t=0) = \frac{3\xi^2}{2m\sqrt{1+\xi^2}} \frac{\mathcal{E}_{\text{cr}}}{\mathcal{E}}, \quad (19)$$

$$p(t=0) = \frac{m\xi^2}{2\sqrt{1+\xi^2}},$$

and the barrier width is $r(0) \gg 1/m$ and momentum $\mathbf{p}(0)$ is perpendicular to fields \mathcal{E} and \mathcal{H} (in contrast to the one-dimensional quasi-classical case, the point of exit from the barrier is no longer the point of particle stop). The ionization rate of the relativistic s th level is (to an accuracy of preexponential factor)

$$w_R \propto \exp\left(-\frac{2\sqrt{3}\xi^3}{1+\xi^2} \frac{\mathcal{E}_{\text{cr}}}{\mathcal{E}}\right). \quad (20)$$

Since the crossed field does not generate pairs, probability w_R differs from zero because there exists a preferred reference system in which the atom is at rest.

¹See, e.g., Eqs. (2.2)–(2.8) in [47]. The formulas for the general case of a monochromatic electromagnetic wave with frequency ω and electric polarization ρ are more complex [42, 50].

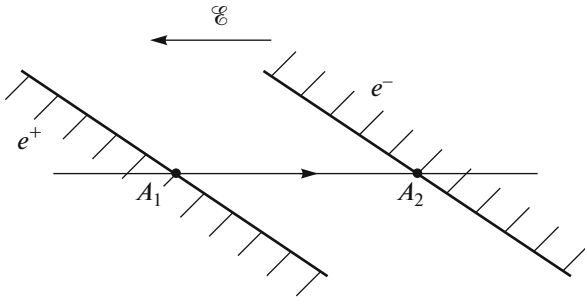


Fig. 1. Upper and lower continua for the Dirac equation in the presence of constant electric field \mathcal{E} . The subbarrier part of the trajectory corresponds to the line connecting turning points A_1A_2 .

3. PAIR PRODUCTION FROM VACUUM IN AN APPLIED ELECTROMAGNETIC FIELD

3.1. Pair Production in a Constant Electric Field

Pair production can be clearly interpreted as the tunneling of an electron from an occupied level lying in the lower continuum (“Dirac sea” filled with electrons with negative energy [1]) through gap $2mc^2$ to one of the vacancy states in the upper continuum (path A_1A_2 in Fig. 1). In constant electric field \mathcal{E} , energy $E = (p^2 + m^2)^{1/2} - e\mathcal{E}x$ and momentum \mathbf{p}_\perp transverse to the applied field are retained. Figure 1 shows the spectrum of possible values of E .

The motion of a relativistic charged particle is described by the formulas [44]

$$p = e\mathcal{E}t, \quad x = (p^2 + m^2)^{1/2}/e\mathcal{E} + \text{const}, \quad (21)$$

$$S = \int_0^t (-m\sqrt{1-v^2} + e\mathcal{E}x) dt \quad (22)$$

$$= \frac{1}{2e\mathcal{E}} \{ p(p^2 + m^2)^{1/2} - m^2 \ln[p + (p^2 + m^2)^{1/2}] \},$$

where S is the action function. Electron energy $(p^2 + m^2)^{1/2}$ is $-m$ at point A_1 and $+m$ at point A_2 . Time ray $(0, +\infty)$ in Fig. 2 corresponds to outgoing electrons, ray $(0, -\infty)$ corresponds to positrons (which move in the opposite time direction, according to the Dirac theory), and subbarrier trajectory segment between points A_1 and A_2 corresponds to a change in “imaginary time” t along loop C enveloping point of branching t_0 of the action function ($p(t_0) = \pm im$).

The increment of the imaginary part of action along C is

$$\Delta S = S_2 - S_1 = i\pi m^2/2e\mathcal{E} \quad (23)$$

(only the logarithm-containing term in Eq. (22) contributes to ΔS). As a result, we obtain the following well-known estimate for the tunneling probability, i.e., the generation of an e^+e^- pair from vacuum by a constant electric field [8, 9]:

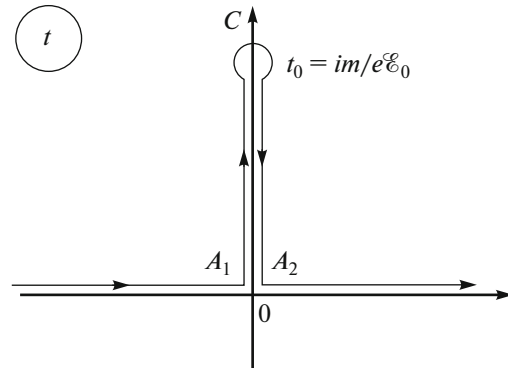


Fig. 2. Change in the imaginary time when an electron moves along the subbarrier trajectory between points A_1 and A_2 . The arrows indicate the direction of changing the complex time during tunneling.

$$w \propto \exp\left(-\frac{2}{\hbar} \text{Im} \Delta S\right) = \exp\left(-\frac{\pi m^2}{e\mathcal{E}}\right) \equiv \exp\left(-\frac{\pi \mathcal{E}_{\text{cr}}}{\mathcal{E}}\right). \quad (24)$$

At $\mathcal{E} \ll \mathcal{E}_{\text{cr}}$, the barrier width (i.e., the distance between points A_1 and A_2) is

$$b = 2m/e\mathcal{E} \sim l_C \mathcal{E}_{\text{cr}}/\mathcal{E} \gg l_C = 1/m, \quad (25)$$

therefore, probability (24) is exponentially small. Once e^+ and e^- leave the barrier at points A_1 and A_2 , respectively, they are accelerated by an electric field in opposite directions, $\mathbf{p}_{e^+} = -\mathbf{p}_{e^-}$.

3.2. Pair Production in an Alternating Electric Field

It is unlikely that the constant electric fields comparable with \mathcal{E}_{cr} will be ever created under laboratory conditions. Therefore, the authors of many theoretical works [28, 29, 32, 51] considered pair production in a linearly polarized alternating field of the form

$$\mathcal{E}(\theta) = \{\mathcal{E}_0 \varphi(\theta), 0, 0\}, \quad \mathcal{H}(\theta) \equiv 0, \quad \theta = \omega t, \quad (26)$$

where, in particular, $\varphi(\theta) = \cos\theta$ in [28, 29, 51] and $\varphi(\theta) = 1/\cosh^2\theta$ in [52]. Here, \mathcal{E}_0 is the field amplitude, t is the time, θ is the dimensionless time, ω is the characteristic frequency, and function $\varphi(\theta)$ specifies a laser pulse shape.

To calculate probability w in model (26), it is convenient to use ITM. In the case of field (26), the subbarrier electron trajectory in vacuum that connects the upper and lower continua is obtained in quadratures. Using this trajectory, we can easily find the probability of production of an e^+e^- pair with momenta $\pm \mathbf{p}$ [28, 29],

$$w(\mathbf{p}) \propto \exp\left\{-\frac{\pi}{\epsilon} \left[\tilde{g}(\gamma_0) + \tilde{b}_\parallel(\gamma_0) \frac{p_\parallel^2}{m^2} + \tilde{b}_\perp(\gamma_0) \frac{p_\perp^2}{m^2} \right]\right\}, \quad (27)$$

where $\epsilon = \mathcal{E}_0/\mathcal{E}_{cr}$ is the reduced electric field and γ_0 is the relativistic adiabaticity parameter, which is analogous to the Keldysh parameter in the nonrelativistic theory of ionization,

$$\gamma_0 = \frac{\omega}{\omega_i} = \frac{mc\omega}{e\mathcal{E}_0} = \frac{\hbar\omega}{e\mathcal{E}_0 l_C} = \frac{\hbar\omega}{mc^2} \frac{\mathcal{E}_{cr}}{\mathcal{E}_0}. \quad (28)$$

Here, $\omega_i \sim 1/T_i$ and $T_i \sim b/c$ are the characteristic electron frequency and tunneling time. Function $\tilde{g}(\gamma)$ and pulsed spectrum coefficients \tilde{b}_{\parallel} and \tilde{b}_{\perp} of are determined by pulse shape $\varphi(\theta)$, and the corresponding formulas are given in [27–29, 32]. Let us present them for several simplest cases.

1. For a monochromatic field with linear polarization $\mathcal{E}(t) = \mathcal{E}_0 \cos\theta$, we have

$$\tilde{g}(\gamma_0) = \frac{4}{\pi} \int_0^1 du \frac{\sqrt{1-u^2}}{\sqrt{1-\gamma_0^2 u^2}} = \frac{4}{\pi\sqrt{1+\gamma_0^2}} \mathbf{D}(q), \quad (29)$$

$$\tilde{b}_{\parallel}(\gamma_0) = \frac{\pi\gamma_0^2}{2(1+\gamma_0^2)} \tilde{g}(\gamma_0) = \frac{2\gamma_0^2}{(1+\gamma_0^2)^{3/2}} \mathbf{D}(q), \quad (30)$$

$$\tilde{b}_{\perp}(\gamma_0) = \frac{2}{\pi\sqrt{1+\gamma_0^2}} \mathbf{K}(q), \quad q = \frac{\gamma_0}{\sqrt{1+\gamma_0^2}},$$

where \mathbf{K} and \mathbf{D} are the complete elliptic integrals of the first and third kind [53]. The total production of pair production in invariant Compton 4-volume, $l_C^4/c \sim 10^{-53} \text{ cm}^3 \text{ s}^{-1}$, is obtained by the integration of Eq. (27) with respect to d^3p and pulse duration τ with allowance for the preexponential factor and the law of conservation of energy in n photon absorption [31].

For optical (and even X-ray) lasers, we have $\hbar\omega \ll mc^2$; therefore, pair production is possible only in the adiabatic range $\gamma_0 \ll 1$, where the formulas are simplified and close to the case of a constant field,

$$w = 3.6 \times 10^{-3} m^4 \epsilon^{5/2} \exp\left\{-\frac{\pi}{\epsilon} \tilde{g}(\gamma_0)\right\}, \quad \epsilon \ll 1, \quad (31)$$

$$\tilde{g}(\gamma_0) = 1 - \frac{1}{8}\gamma_0^2 + \frac{3}{64}\gamma_0^4 + \dots,$$

$$\tilde{b}_{\parallel}(\gamma_0) = \frac{1}{2}\gamma_0^2, \quad \tilde{b}_{\perp} = 1 - \frac{1}{4}\gamma_0^2.$$

The opposite case ($\gamma_0 \gg 1$) can take place only after the creation of γ lasers (which is likely not to be the case of the near future). In this case, we have $\tilde{g}(\gamma_0) = 4(\ln 4\gamma_0 - 1)$ and the pair production probability is represented as the sum of the probabilities of n -photon processes,

$$w = \sum_{n=K_0}^{\infty} w_n, \quad \frac{w_{n+1}}{w_n} \sim \gamma_0^{-2K_0}, \quad (32)$$

where $K_0 = 2m/\omega$ is the multiquantum parameter (i.e., the minimum number of absorbed quanta that is necessary for the production of an e^+e^- pair).

2. For pulsed field $\mathcal{E}(t) = \mathcal{E}_0(1 + \theta^2)^{-3/2}$, we have

$$\tilde{g}(\gamma_0) = \frac{4}{\pi} \int_0^1 du \frac{\sqrt{1-u^2}}{(1+\gamma_0^2 u^2)^{3/2}} = \frac{4}{\pi\sqrt{1+\gamma_0^2}} [\mathbf{K}(q) - \mathbf{D}(q)], \quad (33)$$

where

$$\tilde{g}(\gamma_0) = \begin{cases} 1 - \frac{3}{8}\gamma_0^2 + \frac{15}{64}\gamma_0^4 + \dots, & \gamma_0 \ll 1, \\ \frac{4}{\pi\gamma_0} [1 - \ln(4e\gamma_0)/2\gamma_0^2], & \gamma_0 \gg 1. \end{cases} \quad (34)$$

3. Another example allowing for an analytical solution with ITM is “soliton-like” momentum $\varphi(t) = 1/\cosh^2\theta$ [52], where

$$\tilde{g}(\gamma_0) = \frac{4}{\pi} \int_0^1 du \frac{\sqrt{1-u^2}}{1+\gamma_0^2 u^2} = \frac{2}{1+\sqrt{1+\gamma_0^2}} \quad (35)$$

$$= 1 - \frac{1}{4}\gamma_0^2 + \frac{1}{8}\gamma_0^4 + \dots,$$

$$\tilde{b}_{\parallel} = \frac{\gamma_0^2}{(1+\gamma_0^2)^{3/2}}, \quad \tilde{b}_{\perp} = \frac{1}{\sqrt{1+\gamma_0^2}}. \quad (36)$$

Note that Eqs. (35) and (36) derived using ITM agree with the exact solution to the Dirac equation [54] in the quasi-classical limit

$$\epsilon \ll 1, \quad \omega \ll m, \quad b \gg l_C \quad (37)$$

Other examples of calculating the functions entering into Eq. (27) can be found in [32]. In the examples under study, function $\tilde{g}(\gamma_0)$ decreases with increasing γ_0 and probability w increases sharply (at a fixed field amplitude $\mathcal{E} \ll \mathcal{E}_{cr}$). As in the case of multiphoton atom ionization, this effect manifests itself at high frequencies $\omega \gg \omega_i$, which is explained by a decrease in the effective barrier width in terms of ITM. On the whole, the model case of alternating fields of type (26) can be considered in detail.

Let us present some estimates for model (26) with $\varphi(\theta) = \cos\theta$, i.e., in the case of a monochromatic field. The number of pairs formed in volume² $V = \lambda^3$ for pulse duration τ is $N = w\lambda^3\tau$, where w is probability (24). Figure 3 shows the electric fields required to produce one pair. Here, curves 1 and 5 correspond to a pulse duration $\tau = 2\pi/\omega$ (one field period) and $\tau = 1$ s, respectively, and the values of λ cover the range from 10 600 nm ($\hbar\omega = 0.11$ eV, CO₂ laser) to 13 nm ($\hbar\omega = 95$ eV, free electron laser). For infrared and optical lasers, the pair production threshold is reached at $\mathcal{E} \approx (0.7-1) \times 10^{15}$ W/cm, which is lower than \mathcal{E}_{cr} by one and a half order of magnitude. Figure 4 shows the number of pairs produced in volume $V = \lambda^3$ as a function of the titanium–sapphire laser field amplitude.

²The diffraction limit for the focusing of laser light with wavelength λ .

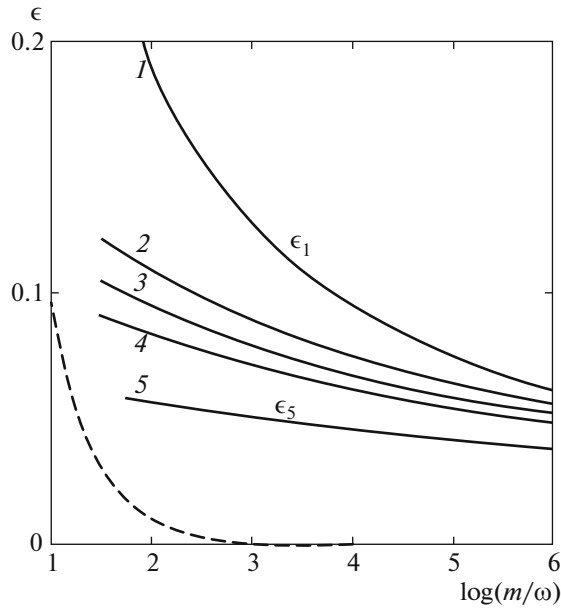


Fig. 3. Reduced electric field $\epsilon = \mathcal{E}_0/\mathcal{E}_{cr}$ that is necessary for the production of one e^+e^- pair in volume $V = \lambda^3$. The curves (in an ascending order) correspond to a pulse duration of 2.6 fs, 0.01 ps, 1 ps, 100 ps, and 1 ns. An adiabaticity region is above the dashed line (for which $\gamma_0 = 1$) [32].

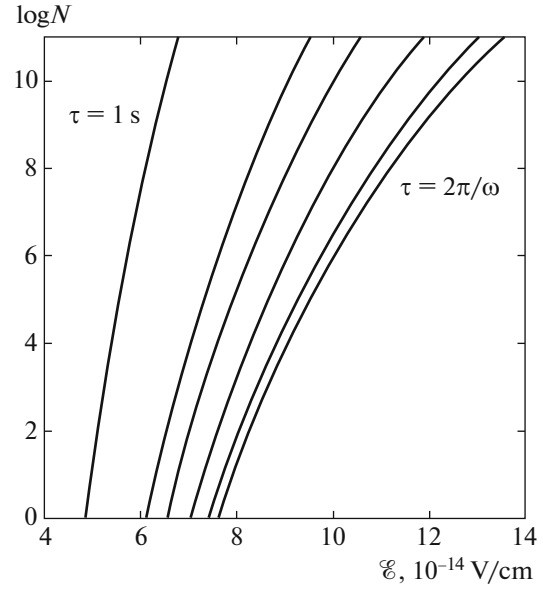


Fig. 4. Number of e^+e^- pairs produced in volume $V = \lambda^3$ vs. the field amplitude for a titanium-sapphire laser ($\lambda = 795$ nm). The curves (from right to left) correspond to a pulse duration $\tau = 2\pi/\omega = 2.6 \times 10^{-15}$, 10^{-14} , 10^{-12} , 10^{-10} , 10^{-8} , and 1 s [32].

Note that these estimates are based on the simplest model of a laser pulse (Eq. (26)) and have a qualitative character.

A comparison of Eq. (27) with Eq. (4.4) from [31] demonstrates that they are analogous and functions g and \tilde{g} analytically differ substantially (therefore, the functions entering into Eq. (27) are denoted by tilde). This difference is explained by different forms of dispersion law $\epsilon(p)$ in Newtonian mechanics and relativistic mechanics. Adiabaticity parameters γ and γ_0 in these two cases also have different orders of magnitude.

Note that, apart from the ionization of atoms and atomic ions, Keldysh [34] also developed a theory for the multiphoton ionization of semiconductors. The dispersion law was chosen as $\epsilon(p) = \Delta(1 + p^2/m_*\Delta)^{1/2}$, where p is the quasi-momentum, m_* is the reduced electron or hole mass, and Δ is the energy gap separating the valence and conduction bands. The expression for $\epsilon(p)$ coincides with the dispersion law $\epsilon(p) = \sqrt{p^2 + m^2}$ in the relativistic quantum mechanics of a free particle up to designations; therefore, the formulas for probability $w(\mathbf{p})$ in these two cases have an analogous form. In this connection, let us also note the Franz-Keldysh effect [55, 56], which consists in a shift in the fundamental absorption edge of light with frequency ω in a semiconductor placed in applied electric field \mathcal{E} . Due to electron tunneling from the valence band to the conduction band, the continuum

boundary diffuses; light with frequency $\omega < \omega_0 = \Delta/\hbar$ can be absorbed; and absorption coefficient $\alpha(\mathcal{E}, \omega)$ has the same form as the tunneling probability (Eq. (24))³ with an exponential accuracy,

$$\alpha(\mathcal{E}, \omega) \propto \exp\left(-\frac{\mathcal{E}_{\text{eff}}}{\mathcal{E}}\right), \quad \mathcal{E}_{\text{eff}} = \frac{4\sqrt{2m_*\hbar}}{3e}(\omega_0 - \omega)^{3/2}. \quad (38)$$

3.3. Pair Production in the Field of a Focused Laser Pulse

Alternating electric field of type (26) with $\mathcal{H} \equiv 0$ is an idealization, which overestimates the number of formed pairs $N_{e^+e^-}$. A real electromagnetic wave always has the magnetic field that decreases $N_{e^+e^-}$ (pairs are known not to be produced in vacuum in a pure magnetic field, as in a plane wave of an arbitrary intensity, polarization, and spectral composition [9, 11]). The authors of [57] considered a realistic three-dimensional model for a focused laser pulse. This model is based on an exact solution to Maxwell's equations in vacuum and contains the following parameters: focal spot radius R , focusing parameter $\Delta = c/\omega R = \lambda/2\pi R$ (which characterizes the difference of a laser pulse from a plane wave), and diffraction

³ See, for example, Section 8, Part VIII in the book by A.I. Anselm *Introduction to the Theory of Semiconductors* (Nauka, Moscow, 1978).

Table 2. Average number of pairs $N_{e^+e^-}$ produced by a single laser pulse of an electric type vs. intensity \mathcal{F} and focusing parameter Δ

\mathcal{F} , 10^{-28} W/cm ²	$\epsilon \times 100$	$N_e, \Delta = 0.1$	$N_e, \Delta = 0.05$
0.4	0.160	0.093	–
0.5	0.179	2.4(1)	–
0.7	0.211	3.8(4)	–
0.8	0.23	5.3(5)	6.4(–11)
0.9	0.240	4.7(6)	4.1(–9)
1.0	0.252	3.0(7)	1.4(–7)
1.5	0.309	1.7(10)	0.023
2.0	0.357	8.0(11)	32
2.5	0.399	1.2(13)	4.6(3)
3.0	0.438	8.4(13)	1.9(5)
5.0	0.565	1.0(16)	1.3(9)

(or Rayleigh) length $L = R/\Delta = kR^2$ ($k = 2\pi/\lambda$ is the wavevector). Note that Δ is a small parameter: in any case, $\Delta \lesssim 1/\pi$. Explicit expressions for the electric field of such a pulse are presented in Appendix C.

To calculate the number of pairs $N_{e^+e^-}$, we take into account that formation length l_f in pair production by a field with a near-critical strength is determined by the Compton length $l_C = \hbar/mc$ [11], which is shorter than the laser radiation wavelength by many orders of magnitude ($l_C \ll \lambda$). Therefore, we may locally use the formula [11] for the average number of pairs produced by a constant electromagnetic field per unit volume and unit time, and the integral of this formula over focal region volume V and pulse duration T gives the total number of produced pairs,

$$N_{e^+e^-} = \frac{1}{4\pi^2 l_C^4} \int dt dV \epsilon(\mathbf{r}, t) \eta(\mathbf{r}, t) \times \coth\left(\frac{\pi \eta(\mathbf{r}, t)}{\epsilon(\mathbf{r}, t)}\right) \exp\left(-\frac{\pi}{\epsilon(\mathbf{r}, t)}\right). \quad (39)$$

Here, $\epsilon(\mathbf{r}, t) = E(\mathbf{r}, t)/\mathcal{E}_{\text{cr}}$ and $\eta(\mathbf{r}, t) = H(\mathbf{r}, t)/\mathcal{E}_{\text{cr}}$ are the local values of invariants E and H normalized by \mathcal{E}_{cr} and having the meaning of the electric field and the magnetic field in the frame of reference where they are parallel to each other,⁴

$$E = \sqrt{(\mathcal{F}^2 + \mathcal{G}^2)^{1/2} + \mathcal{F}}, \quad H = \sqrt{(\mathcal{F}^2 + \mathcal{G}^2)^{1/2} - \mathcal{F}},$$

$$\mathcal{F} = (\mathcal{E}^2 - \mathcal{H}^2)/2, \quad \mathcal{G} = \mathcal{E} \cdot \mathcal{H}.$$

⁴ It is known [44] that such a system always exists except for the case of crossed fields (in this case, however, $\mathcal{F} = \mathcal{G} = 0$ at every point and no pair production takes place).

Explicit expressions for invariants \mathcal{F} and \mathcal{G} and fields \mathcal{E} and \mathcal{H} for this model are given in [57] (see Eqs. (2.1)–(2.12) here).

Note that formation length l_f depends on the field strength as $l_f \sim l_C (\mathcal{E}_{\text{cr}}/\mathcal{E})^{3/2}$ [11]. The locally constant field (LCF) approximation, which serves as the basis of Eq. (39), holds true provided $l_f \ll \lambda$, where λ is the laser pulse wavelength. For a peak field strength, this condition looks like $\mathcal{E}_0 \gg \mathcal{E}_{\text{cr}} (l_C/\lambda)^{2/3}$. This means that the intensity for an optical laser ($\lambda \sim 1 \mu\text{m}$) should be much higher than 10^{21} W/cm². In other words, the LCF approximation is applicable in advance for any field producing pairs.

We now estimate the number of laser-pulse-produced pairs on the assumption that invariant ϵ has a single maximum at the very center of the focal region and magnetic field η vanishes at this point. A similar situation takes place for a focused laser pulse of an electric type (see Appendix C). Then, the main contribution to integral (39) is made by the vicinity of the center of the focal region, where normalized invariants $\epsilon(\mathbf{r}, t)$ and $\eta(\mathbf{r}, t)$ can be written in the form

$$\epsilon(\mathbf{r}, t) \approx \frac{\mathcal{E}_0}{\mathcal{E}_{\text{cr}}} \left(1 - \frac{r_{\perp}^2}{2R^2} - \frac{z^2}{2L^2} - \frac{t^2}{2\tau^2}\right), \quad (40)$$

$$\eta(\mathbf{r}, t) \approx 0,$$

where parameters R and L were determined above and τ is the pulse duration. After simple calculations performed for the total number of produced pairs in this particular case, we obtain

$$N_{e^+e^-} \approx \frac{R^2 L \tau}{\pi^3 l_C^4} \left(\frac{\mathcal{E}_0}{\mathcal{E}_{\text{cr}}}\right)^0 \exp\left(-\frac{\pi \mathcal{E}_{\text{cr}}}{\mathcal{E}_0}\right). \quad (41)$$

At $R \sim \lambda \sim 1 \mu\text{m}$, $L \sim 3\lambda$, and $\tau \sim 10$ fs, the number of pairs $N_{e^+e^-}$ is seen to become on the order of unity at $\mathcal{E}_0 \approx 5.6 \times 10^{-2} \mathcal{E}_{\text{cr}}$. This means that one pair is produced in one shot at an intensity $\mathcal{F} \approx 1.5 \times 10^{27}$ W/cm². This intensity is taken to be the threshold intensity and it is at least two orders of magnitude lower than critical intensity (1).

It has long been thought that the pair production probability is completely determined by the so-called Schwinger exponent $\exp(-\pi \mathcal{E}_{\text{cr}}/\mathcal{E})$ and, hence, is exponentially small at $\mathcal{E} < \mathcal{E}_{\text{cr}}$. However, as is seen from Eq. (41), the Schwinger exponent for the number of produced pairs is accompanied by preexponential factor $V\tau/l_C^4$. This means that the Schwinger exponent determines the pair production probability in the Compton 4-volume l_C^4 . Since the 4-volume $V\tau$ occupied by an electric field is much larger than the Compton volume in any realistic situation, this probability acquires a huge preexponential factor. This factor turns out to be on the order of 10^{25} for an optical laser pulse with a wavelength $\lambda = 1 \mu\text{m}$ and a duration of

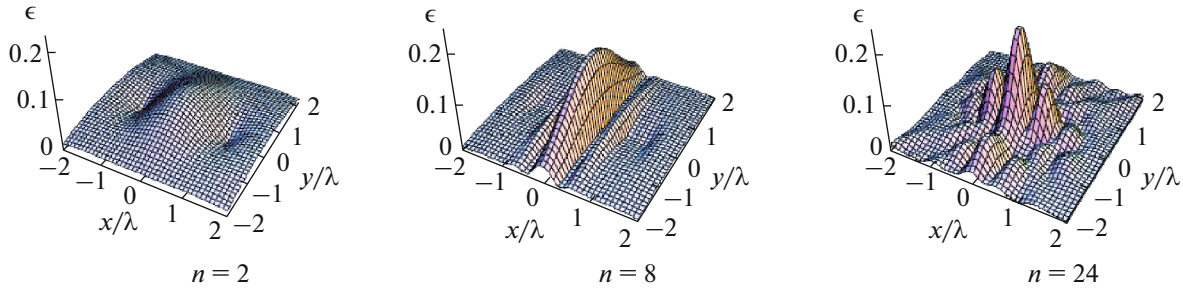


Fig. 5. (Color online) Invariant electric field distribution as a function of the coordinates in plane xy passing through a laser focus for 2, 8, and 24 colliding pulses of an electric type. The total beam power is assumed to be the same in all three cases [58].

10 fs that is focused to the optical limit. This factor is so high that it can compensate for the smallness of the Schwinger exponent even at $\mathcal{E}_0 \ll \mathcal{E}_{\text{cr}}$.

Table 2 gives the results of numerical calculations of the number of pairs $N_{e^+e^-}$ produced by a single focused laser pulse of an electric type as a function of intensity \mathcal{I} and focusing parameter Δ (see Appendix C). As would be expected, the number of produced pairs at the same intensity depends very sharply on the focusing parameter: as it increases twofold, the number of produced pairs increases by more than ten orders of magnitude. The main point, however, is the sharp dependence on the intensity: as the peak intensity grows, the number of produced pairs increases so fast that their rest energy $W_{e^+e^-}^r \approx 2mc^2N_{e^+e^-}$ becomes comparable with laser pulse energy W_L . Moreover, energy $W_{e^+e^-}^r$ becomes much higher than W_L at $\mathcal{E}_0 \sim \mathcal{E}_{\text{cr}}$. This means the following. First, since pairs form at the expense of the laser pulse energy, the process of their production exhausts the laser pulse. Second, the calculation method where a laser field is considered as a given classical external field becomes self-contradictory, since it becomes necessary to take into account the reverse effect of pair production on pulse focusing. Third, the analysis directly indicates that the electric fields on the order of \mathcal{E}_{cr} cannot be achieved for the field that produces electron–positron pairs. The last result is a cogent argument for this statement, which was made by Bohr as early as the 1930s (see, e.g., [5], p. 232).

The threshold intensity can be decreased by using a multibeam technology. As a result of the interference of colliding coherent pulses, the resulting field acquires a spiking space–time structure, which can lead to the fact that the peak field increases and the total field-occupied 4-volume decreases. As the peak field increases, the number of produced pairs grows exponentially; as the field-occupied volume, it decreases but according to a power law. This behavior explains why the threshold intensity decreases. For example, two identical linearly polarized laser pulses can “collide” so that the electric fields are summed up

at the antinodes of the forming standing wave and the magnetic fields compensate each other there.

The number of pairs produced in the field of two colliding pulses was estimated and given in Table 2 in [58]. The aperture of the laser beams limits the number of such pairs in the group consisting of the beams focused onto one point so that their propagation directions lie in the same plane to a certain number $n/2$, where n is the total number of colliding pulses. In this case, the peak strength at the focus increases by a factor of \sqrt{n} . The authors of [59] proposed an optimum configuration for an experiment in which three groups of eight pulses colliding in one plane were used. The propagation direction of the pulses of each group makes an angle $\pi/4$ with the planes of other groups. Figure 5 shows the distribution of invariant electric field ϵ as a function of coordinate in one of the plans passing through the focus for 2, 8, and 24 colliding pulses. According to calculations, the total threshold energy of 24 pulses that is required for the production effect to be detected in this configuration is about 5 kJ for pulses with $\lambda \approx 1 \mu\text{m}$ and a duration of 10 fs. This energy corresponds to the total power of about 500 pW, which is likely to be achieved in the ELI and XCELS plants [17, 18].

3.4. Dynamic Schwinger Effect

We now consider the influence of pulse shortening on the pair production probability and the pulse spectrum of pairs. To this end, it is sufficient to determine the quantities entering into Eq. (27). In particular, we have

$$\tilde{g}(\gamma_0) = \frac{4}{\pi} \int_0^1 \chi(\gamma_0 u) \sqrt{1-u^2} du, \quad (42)$$

where $\chi(u)$ is the auxiliary function unambiguously determined from laser pulse shape $\varphi(\theta)$ and having the form that is identical to that in the theory of multiphoton atomic ionization (see, e.g., section 3 in review [27]) and adiabaticity parameter γ_0 is determined by Eq. (28) (also see Appendix B). If function $\chi(u)$ is

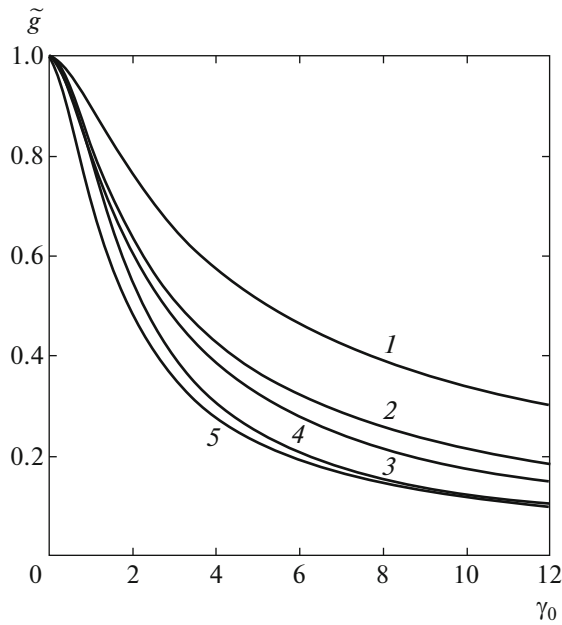


Fig. 6. Function \tilde{g} from Eqs. (27), (42) vs. adiabaticity parameter γ_0 for pulses of various shapes: (1) $\varphi = \cos\theta$, (2) $\varphi = \exp(-\theta^2)$, (3) $\varphi = 1/\cosh^2\theta$, (4) $\varphi = (1 + \theta^2)^{-1}$, and (5) $\varphi = (1 + \theta^2)^{-2}$ ($\theta = \omega t$).

known, the calculation of the pair production probability and the pulse spectrum of pairs is reduced to quadrature. The calculation results are shown in Fig. 6. Curves 1–5 belong to the fields of the following types: (1) $\varphi = \cos\theta$ (monochromatic pulse), (2) $\varphi = \exp(-\theta^2)$ (Gaussian), (3) $\varphi = 1/\cosh^2\theta$ (soliton-like pulse [52]), (4) $\varphi = (1 + \theta^2)^{-1}$ (Lorentzian pulse), and (5) $\varphi = (1 + \theta^2)^{-2}$. In all cases, function $\tilde{g}(\gamma_0)$ decreases monotonically with increasing adiabaticity parameter, and probability w grows sharply (at a fixed field $\mathcal{E} \ll \mathcal{E}_{cr}$) and depends substantially on the laser pulse shape at $\gamma_0 \gtrsim 1$. This phenomenon appears at high frequencies $\omega \gtrsim \omega_r$, is analogous to the behavior of the probability of multiphoton atomic ionization as a function of Keldysh parameter γ , and was called dynamic Schwinger effect [32].

For modern lasers, we have $\hbar\omega \ll mc^2$; therefore, we present the expansions of the functions entering into Eq. (27) at $\gamma_0 \ll 1$. In the adiabatic region, the probability is mainly determined by the behavior of the field near the maximum. Without loss of generality, we assume that the maximum of field $\mathcal{E}(\theta)$ is reached at $\theta = 0$ and $\varphi(0) = 1$, so that

$$\varphi(\theta) = 1 - \frac{a_2}{2!}\theta^2 + \frac{a_4}{4!}\theta^4 + \dots, \quad a_2 > 0, \quad (43)$$

and obtain

$$\begin{aligned} \tilde{g}(\gamma_0) &= 1 - \frac{1}{8}a_2\gamma_0^2 + \frac{1}{192}(10a_2^2 - a_4)\gamma_0^4 + \mathcal{O}(\gamma_0^6), \\ \tilde{b}_{\parallel} &= \frac{1}{2}a_2\gamma_0^2 + \dots, \quad \tilde{b}_{\perp} = 1 - \frac{1}{8}\gamma_0^2 + \dots \end{aligned} \quad (44)$$

Along with Eqs. (27) and (31), these expressions determine the pair production probability in the low-frequency limit.

4. GROUP-THEORETICAL ASPECT OF THE PROBLEM OF PAIR PRODUCTION

4.1. Boson Case ($s = 0$)

In the calibration $\mathbf{A} = 0$ and $A_0 = -\mathcal{E}(t) \cdot \mathbf{r}$, the Klein–Fock–Gordon equation has the solution

$$\psi(\mathbf{r}, t) = \xi(t)e^{i\mathbf{p}\cdot\mathbf{r}}, \quad (45)$$

where \mathbf{p} is the momentum of a classical particle in field $\mathcal{E}(t)$,

$$\mathbf{p}(t) = \mathbf{p}_- + e \int_{-\infty}^t \mathcal{E}(t') dt' = \mathbf{p}_+ - e \int_t^{\infty} \mathcal{E}(t') dt', \quad (46)$$

and function $\xi(t)$ satisfies the oscillator equation

$$\begin{aligned} \ddot{\xi} + \omega^2(t)\xi &= 0, \quad \omega^2(t) = m^2 + p^2(t), \\ \lim_{t \rightarrow \pm\infty} \omega(t) &= (m^2 + p_{\pm}^2)^{1/2} \equiv \omega_{\pm}. \end{aligned} \quad (47)$$

The electric field vanishes at infinity, which makes it possible to formulate the problem of pair production from vacuum mathematically correctly.

When passing from the Schrödinger to the Heisenberg representation, we have

$$\psi(\mathbf{r}, t) = \sum_{\mathbf{p}} \frac{\exp(i\mathbf{p}(t) \cdot \mathbf{r})}{\sqrt{2\omega_-}} [\hat{a}_{\mathbf{p}}(t) + \hat{b}_{-\mathbf{p}}^{\dagger}(t)]. \quad (48)$$

Here, the Bogoliubov canonical transformation

$$\begin{aligned} \hat{a}_{\mathbf{p}}(t) &= u(t)a_{\mathbf{p}} + v(t)b_{-\mathbf{p}}^{\dagger}, \\ \hat{b}_{-\mathbf{p}}^{\dagger}(t) &= v^*(t)a_{\mathbf{p}} + u^*(t)b_{-\mathbf{p}}^{\dagger} \end{aligned} \quad (49)$$

holds, and its coefficients can be expressed in terms of the solution to oscillator equation (47). For example, at $t \rightarrow -\infty$, we have

$$\begin{aligned} \omega(t) &\rightarrow \omega_-, \quad u(t) = \exp(-i\omega_- t), \quad v(t) = 0, \\ \hat{a}_{\mathbf{p}}(t) &= a_{\mathbf{p}} \exp(-i\omega_- t), \end{aligned} \quad (50)$$

The conservation of the commutator between Heisenberg operators in time,

$$[\hat{a}_{\mathbf{p}}(t), \hat{a}_{\mathbf{p}}^{\dagger}(t)] = [\hat{b}_{\mathbf{p}}(t), \hat{b}_{\mathbf{p}}^{\dagger}(t)] = \delta(\mathbf{p} - \mathbf{p}'),$$

imposes the condition

$$|u(t)|^2 - |v(t)|^2 = 1, \quad (51)$$

which demonstrates that canonical transformation (49) belongs to quasi-unitary group $SU(1, 1)$. n pairs of

bosons can be in the given quantum state (with momentum $\mathbf{p} = \mathbf{p}(t \rightarrow +\infty)$), and the distribution over the number of pairs has the form

$$w_n = (1 - \rho)\rho^n, \quad n = 0, 1, 2, \dots, \quad (52)$$

where

$$\rho = |C_2/C_1|^2, \quad 0 \leq \rho < 1, \\ \xi(t \rightarrow -\infty) = e^{-i\omega_+ t}, \quad \xi(t \rightarrow +\infty) = C_1 e^{i\omega_+ t} + C_2 e^{-i\omega_+ t}. \quad (53)$$

4.2. Fermion Case ($s = 1/2$)

For fermions with spin $s = 1/2$, from the Dirac equation we obtain

$$i\dot{\xi} = [\boldsymbol{\alpha} \cdot \mathbf{p}(t) + \beta m]\xi, \quad (54)$$

where $\xi(t)$ is a bispinor and $\boldsymbol{\alpha}$ and β are Dirac matrices, instead of Eq. (47). The quantized spinor field operator has the form

$$\Psi_{\alpha}(\mathbf{r}, t) = (2\pi)^{-3/2} \int \frac{d^3 p}{2\omega_-} e^{ip(t) \cdot \mathbf{r}} \\ \times \sum_{\sigma=\pm 1/2} [\hat{a}_{\sigma}(\mathbf{p}, t) u_{\alpha}^{\sigma} + \hat{b}_{\sigma}^{\dagger}(-\mathbf{p}, t) v_{\alpha}^{\sigma}], \quad (55)$$

where \hat{a} and \hat{b} are the Heisenberg annihilation operators for a particle and the antiparticle, respectively, and spinors u and v satisfy the Dirac equations with variable $\mathbf{p}(t)$ and $\varepsilon(t)$,

$$[\boldsymbol{\alpha} \cdot \mathbf{p}(t) + \beta m]u^{\sigma} = \varepsilon(t)u^{\sigma}, \\ [\boldsymbol{\alpha} \cdot \mathbf{p}(t) + \beta m]v^{\sigma} = -\varepsilon(t)v^{\sigma}. \quad (56)$$

As in Eq. (49), the time dependences of operators \hat{a} and \hat{b} are expressed in terms of canonical transformation,

$$\hat{a}(\mathbf{p}, t) = U(t)a(\mathbf{p}, t_0) + \bar{V}^{\dagger}(t)\bar{b}^{\dagger}(-\mathbf{p}, t_0), \\ \hat{b}^{\dagger}(\mathbf{p}, t) = V(t)a(\mathbf{p}, t_0) + \bar{U}^{\dagger}(t)\bar{b}^{\dagger}(-\mathbf{p}, t_0), \quad (57)$$

where U and V are second-order matrices.⁵ Here, we have $U^{\dagger}U + V^{\dagger}V = 1$ and

$$\dot{U} = -i[\varepsilon(t) + N]U - PV, \\ \dot{V} = PU + i[\varepsilon(t) - N]V, \quad (58)$$

where

$$N = \frac{\boldsymbol{\sigma} \cdot \dot{\mathbf{p}}}{\varepsilon(t)[m + \varepsilon(t)]} = \frac{\mathbf{v} \cdot \dot{\mathbf{v}}}{1 + \sqrt{1 - v^2}}, \\ P = \left(\dot{\mathbf{v}}^2 + \frac{(\mathbf{v} \cdot \dot{\mathbf{v}})^2}{1 - v^2} \right)^{1/2}$$

and $\sigma = \pm 1/2$ is the projection of spin. In the nonrelativistic limit, the expression for N changes into the

⁵ Here, we omit the details of calculations (see Chapter 4 in [60] for details).

well-known formula for the Thomas precession, $N = (\mathbf{v} \cdot \dot{\mathbf{v}})/2$.

According to the Pauli principle, 0, 1, or 2 e^+e^- pairs can be in a certain state (\mathbf{p}, σ) with the probabilities

$$w_0 = (1 - v_1)(1 - v_2), \quad w_1 = v_1 + v_2 - 2v_1v_2, \\ w_2 = v_1v_2, \quad (59)$$

where v_i are the eigenvalues of the matrix $V^{\dagger}U(t \rightarrow \infty)$.

In the case of a homogeneous magnetic field $\mathcal{E}(t)$, charged-field oscillators have a time-variable frequency but remain independent. Therefore, only operators $\hat{a}(\mathbf{p}, t)$ and $\hat{b}^{\dagger}(-\mathbf{p}, t)$ (and $\hat{a}^{\dagger}(\mathbf{p}, t)$ and $b(-\mathbf{p}, t)$) are mixed during evolution, which significantly simplifies the solution of the problem.

4.3. The theory of group representations can be used to find the solution in a short and elegant manner. In the problem of pair production from vacuum, $\hat{a}^{\dagger}\hat{b}^{\dagger}$ is obviously a raising operator. Here, \hat{a}^{\dagger} is the particle production operator and \hat{b}^{\dagger} is the antiparticle production operator (indices \mathbf{p} and σ of operators \hat{a} and \hat{b} are omitted here). For bosons, we assume

$$J_0 = \hat{a}^{\dagger}\hat{b}^{\dagger}, \quad J_- = \hat{b}\hat{a} = \hat{a}\hat{b}, \\ J_0 = \frac{1}{2}(\hat{a}^{\dagger}\hat{a} + \hat{b}^{\dagger}\hat{b} + 1), \quad (60)$$

where $[\hat{a}^{\dagger}, \hat{a}] = [\hat{b}^{\dagger}, \hat{b}] = 1$; for the case of fermions (where anticommutators are $\{\hat{a}^{\dagger}, \hat{a}\} = \{\hat{b}^{\dagger}, \hat{b}\} = 1$), we have

$$J_+ = \hat{a}^{\dagger}\hat{b}^{\dagger}, \quad J_- = \hat{b}\hat{a} = -\hat{a}\hat{b}, \\ J_0 = \frac{1}{2}(\hat{a}^{\dagger}\hat{a} + \hat{b}^{\dagger}\hat{b} - 1). \quad (61)$$

We can easily show that

$$[J_0, J_{\pm}] = \pm J_{\pm}, \quad [J_+, J_-] = 2\eta J_0, \quad (62)$$

where $\eta = -1$ in the case of bosons and $\eta = 1$ in the case of fermions. Therefore, operators (60) and (61) are seen to be the generators of groups (more specifically, algebras) $SU(1,1)$ and $SU(2)$, and the Casimir operator ("angular momentum" squared per group) is

$$J^2 = J_0^2 + \eta(J_1^2 + J_2^2) \\ = \frac{2\eta + 1}{4}[1 - (\hat{a}^{\dagger}\hat{a} - \hat{b}^{\dagger}\hat{b})^2]. \quad (63)$$

In the vacuum state, we have $\hat{a}^{\dagger}\hat{a} = \hat{b}^{\dagger}\hat{b} = 0$; therefore, we have

$$J^2 = j(j+1) = -\frac{1}{4}, \quad j = -\frac{1}{2} \quad (64)$$

for bosons and

$$J^2 = j(j+1) = \frac{3}{4}, \quad j = \frac{1}{2} \quad (65)$$

for fermions. The vacuum–vacuum transition probability is the Wigner function squared for the corresponding representation,

$$w_{00} = |d_{-j,-j}^{(j)}(\beta \text{ or } \theta)|^2 = \begin{cases} 1/\cosh^2(\beta/2), & s = 0, \\ \cos^2(\theta/2), & s = 1/2, \end{cases} \quad (66)$$

where β and θ are the “angles of rotation” ($0 < \beta < \infty$ for $SU(1, 1)$ and $0 < \theta < \pi/2$ for $SU(2)$).

4.4. As an example that allows an analytical solution, we choose the pulse

$$\mathcal{E}(t) = \mathcal{E}_0(\cosh \Omega t)^{-2}, \quad (67)$$

which corresponds to the well-known Eckart potential [61]. In this case (for fermions with $s = 1/2$), we have

$$\omega^2(t) = \frac{1}{2}[\omega_+^2 + \omega_-^2 + (\omega_+^2 - \omega_-^2) \tanh \Omega t] - \Omega^2(\kappa^2 \pm i\kappa)(\cosh \Omega t)^{-2}, \quad (68)$$

where $\kappa = e\mathcal{E}_0/\Omega^2$. In this case, we have [30, 60]

$$R_{\pm} = -i \frac{\Gamma(iv_+) \Gamma(1 - iv - ip/2) \Gamma(iv - ip/2)}{\Gamma(-iv_+) \Gamma(1 - iv + i\sigma/2) \Gamma(iv + i\sigma/2)}, \quad (69)$$

where $v_+ + v_- = \pi(\omega_+ + \omega_-)/\Omega$ and $\sigma = v_+ - v_-$. Substituting this expression into the relation $\rho = |R_{\pm}|$, we find

$$\rho_{s=1/2} = \frac{\cosh v - \cosh(v_+ - v_-)}{\cosh(v_+ + v_-) - \cosh v}, \quad (70)$$

$$v_+ + v_- > v > |v_+ - v_-|,$$

where $v_{\pm} = \pi\omega_{\pm}/\Omega$ and $v = 2\pi e\mathcal{E}_0/\Omega^2$. Analogous formulas take place for scalar particles ($s = 0$),

$$\rho_{s=0} = \frac{\cosh(v_+ - v_-) + \cos \sqrt{1 - \kappa^2}}{\cosh(v_+ + v_-) + \cos \sqrt{1 - \kappa^2}}. \quad (71)$$

The formulas that are equivalent to Eqs. (70) and (71) were derived in [54] and were used to find the exact solution to the Dirac and Klein–Fock–Gordon equations for field (67) and to calculate the probability of pair production from vacuum. In our approach, the problem is reduced to the calculation of the transmission coefficient through a one-dimensional potential barrier, and some exact and approximate solutions to this problem can be found in [60]. Note that ITM can be applied to the solution of the problem of pair production by field $\mathcal{E}(t)$ when the conditions

$$\mathcal{E}_0 \ll \mathcal{E}_{\text{cr}}, \quad \hbar\omega \ll mc^2 \quad (72)$$

are met.

If conditions (72) are met, we have

$$v_{\pm} \gg 1, \quad v_+ + v_- \gg v|v_+ - v_-|.$$

When expanding

$$\omega_{\pm} = m \left\{ 1 + \frac{p_{\perp}^2}{m^2} + \left(\gamma^{-1} \pm \frac{p_{\parallel}}{m} \right)^2 \right\}^{1/2}$$

into a series in powers of p/m , we can transform Eqs. (70) and (71) to the form

$$\rho_s(\mathbf{p}) = D \exp \left\{ -\frac{\pi \mathcal{E}_{\text{cr}}}{\mathcal{E}_0} \left[\frac{2}{1 + \sqrt{1 + \gamma_0^2}} + \frac{1}{\sqrt{1 + \gamma_0^2}} \frac{p_{\perp}^2}{m^2} + \frac{\gamma_0^2}{(1 + \gamma_0^2)^{3/2}} \frac{p_{\parallel}^2}{m^2} \right] \right\}, \quad (73)$$

where γ_0 is the adiabaticity parameter (see Eq. (28)) and the preexponential factor is

$$D = \begin{cases} [\exp(-(v - \sqrt{v^2 - 1})) + \exp(-(v + \sqrt{v^2 - 1}))]^2, & s = 0, \\ (1 - \exp(-2v))^2, & s = 1/2. \end{cases} \quad (74)$$

At $\omega \gg m\sqrt{\mathcal{E}_0/\mathcal{E}_{\text{cr}}}$, we have parameter $v \gg 1$ and

$$D \approx \begin{cases} 1 - \mathcal{O}(1/v^2), & s = 0, \\ 1 - \mathcal{O}(e^{-2v}), & s = 1/2. \end{cases} \quad (75)$$

In this case, the probability is almost independent of spin and coincides with the result of the quasi-classical calculation (Eq. (27)), including the preexponential factor.

In conclusion, note that, in the specific case of homogeneous electric field $\mathcal{E}(t)$ that retains its direction in space, the calculation of the probability of pair production from vacuum is reduced to the problem [62] of excitation of a one-dimensional oscillator with variable frequency $\omega(t)$ [30, 60],

$$\omega^2(t) = \begin{cases} m^2 + p^2(t), & s = 0, \\ m^2 + p^2(t) \pm i\mathcal{E}(t), & s = 1/2, \end{cases} \quad (76)$$

with the oscillator frequency being real in the case of bosons and imaginary in the case of fermions.

ACKNOWLEDGMENTS

We thank M.I. Vysotskii for useful discussions.

This work was performed in the Applied Mathematics and Theoretical Physics Center and was supported by the program of increasing the competitive ability of National Research Nuclear University MEPhI (agreement with the Ministry of Education and Science of the Russian Federation of August 27, 2013, project no. 02.a03.21.0005) and the Russian Foundation for Basic Research (project no. 16-02-00936).

APPENDIX A

Adiabatic Expansion

The frequency dependence of the tunneling probability during the ionization of an atomic level by laser radiation or during the production of e^+e^- pairs from

vacuum by field $\mathcal{E}(t)$ is determined by functions $g(\gamma)$ and $\tilde{g}(\gamma_0)$. To within a preexponential factor, we have

$$w(\gamma) \propto \exp\left\{-\frac{2\kappa^2 \mathcal{E}_a}{3\mathcal{E}_0} g(\gamma)\right\}, \quad (\text{A.1})$$

$$\tilde{w}(\gamma_0) \propto \exp\left\{-\frac{2m}{\omega} \tilde{g}(\gamma_0)\right\},$$

where [47, 50]

$$g(\gamma) = \frac{3}{2\gamma_0} \int_0^\gamma \chi(u) \left(1 - \frac{u^2}{\gamma^2}\right) du, \quad (\text{A.2})$$

$$\tilde{g}(\gamma_0) = \frac{4}{\pi\gamma_0} \int_0^{\gamma_0} \chi(u) \left(1 - \frac{u^2}{\gamma_0^2}\right)^{1/2} du,$$

γ (Keldysh parameter [34]) and γ_0 are the adiabaticity parameters for these problems, respectively,

$$\gamma = \frac{\omega\kappa}{\mathcal{E}_0} \quad (\hbar = m = e = 1, \kappa = \sqrt{2I}), \quad (\text{A.3})$$

$$\gamma_0 = \frac{m\omega}{e\mathcal{E}_0} \quad (\hbar = c = 1),$$

I is the ionization potential, and function $\chi(u)$ is determined by laser pulse shape $\varphi(\omega t)$ (see [31, section 4]).

In the case of a low-frequency field ($\gamma, \gamma_0 \ll 1$), it is natural to use the adiabatic expansions

$$g(\gamma) = \sum_0^\infty (-1)^n g_n \gamma^{2n}, \quad (\text{A.4})$$

$$\tilde{g}(\gamma_0) = \sum_0^\infty (-1)^n \tilde{g}_n \gamma_0^{2n}, \quad g(0) = \tilde{g}(0) = 1.$$

The relation between the coefficients of these expansions (at any pulse shape) is found from Eq. (A.2),

$$\frac{\tilde{g}_n}{g_n} = \frac{4}{3(n+1)! \Gamma(1/2)} = 1, \frac{5}{4}, \frac{35}{24}, \dots \quad (\text{A.5})$$

for $n = 0, 1, 2, \dots$. In the case of monochromatic radiation, we obtain

$$g(\gamma) = 1 - \frac{1}{10} \gamma^2 + \frac{9}{280} \gamma^4 - \frac{5}{386} \gamma^6 + \dots,$$

and, with allowance for Eq. (A.5), we have adiabatic expansion for the probability of pair production by field $\varphi(t) = \cos\omega t$,

$$\tilde{g}(\gamma_0) = 1 - \frac{1}{8} \gamma_0^2 + \frac{3}{64} \gamma_0^4 - \frac{175}{768} \gamma_0^6 + \dots \quad (\text{A.6})$$

In the general case, we assume that pulse function $\varphi(\theta)$ has a maximum at zero and $\varphi(0) = 1$, $\varphi'(0) = 0$, $\varphi''(0) < 0$,

$$\varphi(\theta) = 1 - \frac{a_2}{2!} \theta^2 + \frac{a_4}{4!} \theta^4 - \dots, \quad a_2 > 0, \quad \theta = \omega t,$$

and obtain

$$\tilde{g}(\gamma_0) = 1 - \frac{1}{8} a_2 \gamma_0^2 + \frac{1}{192} (10a_2^2 - a_4) \gamma_0^4 + \dots \quad (\text{A.7})$$

A similar expansion takes place for $g(\gamma)$.

APPENDIX B

Parameters γ_r and γ_R

In the nonrelativistic Keldysh theory of ionization [34], the adiabaticity parameter has the form $\gamma = \omega\kappa/\mathcal{E}_0$ ($\hbar = m = e = 1$). The process of ionization is tunneling at $\gamma \ll 1$ and is multiphoton at $\gamma \gg 1$. The choice of a proper adiabaticity parameter in the relativistic case needs explanation.

γ_0 determined in Eq. (28) can be used as a relativistic generalization of this parameter. However, this quantity is independent of the level energy in an atom; therefore, it is inconvenient to describe the process of relativistic ionization (in the case of pair production, rest energy mc^2 is the measure of energy and parameter γ_0 appears naturally). The expression

$$\gamma_r = \frac{m\omega}{\mathcal{E}_0} \sqrt{1 - \epsilon_0^2} \equiv \gamma_0 \sqrt{1 - \epsilon_0^2}, \quad (\text{B.1})$$

could be a level-energy-dependent relativistic generalization of the Keldysh parameter: this expression transforms into the expression for γ in the nonrelativistic limit $\epsilon_0 = E_0/mc^2 \rightarrow 1 - I/mc^2$. However, we have $\gamma_r \rightarrow 0$ at $\epsilon_0 \rightarrow -1$ when a level approaches the boundary of the lower continuum and Eq. (B.1) loses its meaning. This is related to the fact that, at level energies $\epsilon_0 < 0$, the path of integration in the complex time plane changes its form (see Fig. 2).

In terms of ITM, it is natural to take $|t_0|$, where t_0 is the total (purely imaginary) time of subbarrier motion, as the electron tunneling time. In the case of crossed low-frequency fields ($\mathcal{E} = \mathcal{H}$, $\mathcal{E} \perp \mathcal{H}$, $\omega \ll \kappa^2$), a subbarrier trajectory is analytically found. In particular, we have

$$t_0 = i \sqrt{\frac{3\xi^2}{1 + \xi^2} \frac{\mathcal{E}_{cr}}{\mathcal{E}_0}}, \quad \mathbf{r}(t_0) = 0, \quad (\text{B.2})$$

where variable $\xi = \xi(\epsilon_0)$ was determined in Eq. (12). As a result, we obtain

$$\gamma_R = \omega|t_0| = \frac{m\omega}{e\mathcal{E}_0} \sqrt{\frac{3\xi^2}{1 + \xi^2}} = \left(1 - \frac{\xi^2}{3}\right)^{-1/2} \gamma_r. \quad (\text{B.3})$$

At low frequencies, $\omega \rightarrow 0$ (and $\epsilon_0 > 0$), the values of γ_r and γ_R are close to each other. For example, in the model of a hydrogen-like atom (ion) with charge $Z < \alpha^{-1} = 137$, we have $\epsilon_0 = \sqrt{1 - (Z\alpha)^2} = 0.926, 0.899, 0.741$, and 0 and

$$\gamma_r/\gamma_R = 0.997, 0.99, 0.97, 0.816 \quad (\text{B.4})$$

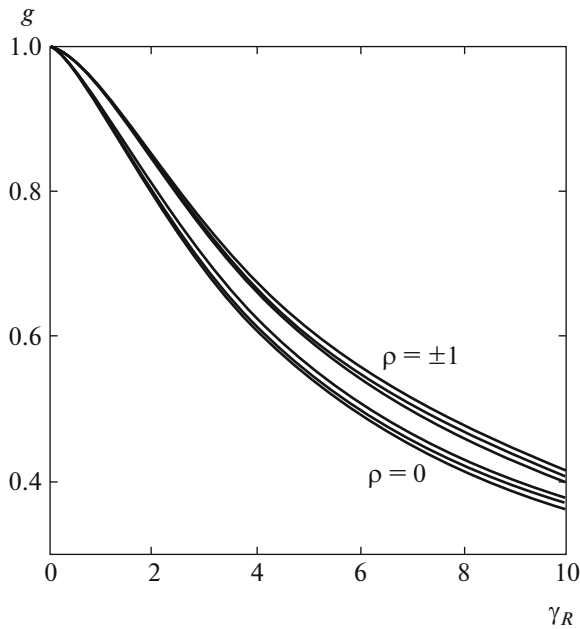


Fig. 7. Function g vs. adiabaticity parameter γ_R . At a given radiation ellipticity ρ , the curves correspond to $\epsilon_0 = 1, 0$, and -1 (from top to bottom) [50].

respectively, at $Z = 30, 60, 92$, and 137 . On the other hand, at $\epsilon_0 \rightarrow -1$, we have $\gamma_r \rightarrow 0$ while γ_R differs from parameter $\gamma_0 = mc\omega/e\mathcal{E}_0$, which appears in the theory of pair production from vacuum in an alternating electric field, only in a numerical factor of 1.224. Figure 7 shows the dependence of function g in the exponent in Eq. (9) on parameter γ_R . The transition from a constant field ($\gamma_R = 0$) to the case of $\gamma_R \gg 1$ leads to a sharp increase in the tunneling probability (as in the theory of multiphoton ionization of atoms), and the numerical values of $g(\gamma_R, \epsilon_0)$ are almost independent of level energy ϵ_0 . Therefore, the choice of a relativistic adiabaticity parameter in form (B.3) seems to be preferable.

APPENDIX C

Three-Dimensional Model of a Focused Laser Pulse

A plane electromagnetic wave with linear polarization is specified by the 4-potential

$$\mathbf{A} = \left(\frac{\mathcal{E}_0}{\omega} a(\varphi), 0, 0 \right), \quad A_0 = 0, \quad (\text{C.1})$$

where $\mathcal{E} = \mathcal{H} = \mathcal{E}_0 da(\varphi)/dt$, $\varphi = \omega(t - z)$ is the light front variable, and axis z is chosen along the wave propagation direction. Function $a(\varphi)$ determines a pulse shape. For example, $a(\varphi) = \sin\varphi$ corresponds to monochromatic laser radiation, $a(\varphi) = \tanh\varphi$ corresponds to a soliton-like pulse $\mathcal{E}(t, z) = \mathcal{E}_0/\cosh^2\varphi$, and so on.

The authors of [57] found exact solutions to Maxwell's equations in vacuum, which are characterized by parameters R (focal spot radius), L (diffraction

length), and Δ (focusing parameter) and describe time-stationary focused laser pulses. They also found approximate solutions, which describe pulses of finite time τ and are characterized by envelope $g(\tau)$.

The electric field in a stationary focused laser pulse of an electric type (where a magnetic field has a non-zero projection on the pulse propagation direction and an electric field lies in plane xy) has the form [57]

$$\mathcal{E}^e = i\mathcal{E}_0 e^{-i\varphi} \{ (\mathbf{e}_x \pm i\mathbf{e}_y) F_1 - e^{2i\varphi} (\mathbf{e}_x \mp i\mathbf{e}_y) F_2 \}, \quad (\text{C.2})$$

where functions F_1 and F_2 are determined from the solution of the equations

$$2i \frac{\partial F_1}{\partial \chi} + \Delta^2 \frac{\partial^2 F_1}{\partial \chi^2} + \frac{1}{\xi} \frac{\partial}{\partial \xi} \left(\xi \frac{\partial F_1}{\partial x} \right) = 0, \quad (\text{C.3})$$

$$F_2 = F_1 - \frac{2}{\chi^2} \int_0^\xi d\xi' \xi' F_1(\xi'),$$

where $\chi = z/L$, $\xi = \rho/R$, $\rho = \sqrt{x^2 + y^2}$, and $\exp(i\varphi) = (x + iy)/\rho$. At $\xi, |\chi| \rightarrow \infty$, we have $F_{1,2} \rightarrow 0$. Focal spot radius R in plane xy , diffraction (Rayleigh) length L , and focusing parameter Δ are related as follows:

$$L = \frac{R}{\Delta} = kR^2, \quad k = \frac{2\pi}{\lambda}. \quad (\text{C.4})$$

The magnetic field of pulse \mathcal{H}^e is described by analogous and more awkward expressions [57].

If a laser pulse is focused to the diffraction limit ($R \sim \lambda$), we have $\Delta \sim 1/2\pi \sim 0.1$; therefore, we assume $\Delta \ll 1$. In this case, functions F_1 and F_2 entering into Eq. (C.2) have the form

$$F_1 = (1 + 2i\chi)^{-2} \left(1 - \frac{\xi^2}{1 + 2i\chi} \right) \exp\left(-\frac{\xi^2}{1 + 2i\chi} \right), \quad (\text{C.5})$$

$$F_2 = -\xi^2 (1 + 2i\chi)^{-3} \exp\left(-\frac{\xi^2}{1 + 2i\chi} \right).$$

Pulses of this type are usually called Gaussian beams.

Another solution to Maxwell's equations is an h -polarized wave, the electric and magnetic fields of which are expressed in terms of the fields of an e -polarized wave according to the equations

$$\mathcal{E}^h = \pm i\mathcal{H}^e, \quad \mathcal{H}^h = \mp i\mathcal{E}^e. \quad (\text{C.6})$$

The superscript corresponds to the left and the subscript, to the right circular polarization of the wave. In this case, the magnetic field is transverse.

To generalize this expression to the case of a nonstationary laser pulse of duration τ , envelope $g(\varphi/\omega\tau)$, which meets the conditions $g(0) = 1$ and $g \rightarrow 0$ at $|\varphi| \gg \omega\tau$, is introduced into Eq. (C.1). Strictly speaking, such functions are not exact solutions to Maxwell's equations: they approximately satisfy them at $\omega\tau \gg 1$. For detailed models of a focused laser pulse, see [57–59].

REFERENCES

1. P. A. M. Dirac, Prog. R. Soc. London A **117**, 610 (1928), Prog. R. Soc. London A **118**, 351 (1928).
2. P. A. M. Dirac, *The Principles of Quantum Mechanics* (Clarendon, Oxford, 1958).
3. W. Gordon, Z. Phys. **48**, 11 (1928).
4. C. G. Darwin, Prog. R. Soc. London, Ser. A **118**, 654 (1928).
5. A. Sommerfeld, *Atombau und Spektrallinien* (Vieweg, Braunschweig, 1939), Vol. 2.
6. F. Sauter, Z. Phys. **69**, 742 (1930); Z. Phys. **73**, 547 (1931).
7. A. Calogeracos and N. Dombey, Contemp. Phys. **40**, 313 (1999).
8. W. Heisenberg and H. Euler, Z. Phys. **98**, 714 (1936).
9. J. Schwinger, Phys. Rev. **82**, 664 (1951).
10. V. S. Vanyashin and M. V. Terent'ev, Sov. Phys. JETP **21**, 375 (1965).
11. A. I. Nikishov, Tr. FIAN **111**, 152 (1979).
12. V. Yanovsky, V. Chvykov, G. Kalinchenko, et al., Opt. Express **16**, 2109 (2008).
13. J. Andruszkow, B. Aunte, V. Ayvazyan, et al., Phys. Rev. Lett. **85**, 3825 (2000).
14. T. Shintake, H. Tanaka, T. Hara, et al., Nature Photon. **2**, 555 (2008).
15. P. Emma, R. Arke, J. Arthur, et al., Nature Photon. **4**, 641 (2010).
16. L. Young, E. P. Kanter, B. Krässig, et al., Nature **466**, 56 (2010).
17. European Project on Extreme Light Infrastructure. <http://www.extreme-light-infrastructure.eu>
18. Exawatt Center for Extreme Light Studies (XCELS) on the Base of Institute of Applied Physics of RAS. <http://www.xcels.iapas.ru>
19. International Center for Zetta-Exawatt Science and Technology (IZEST). <http://www.izest.polytechnique.edu>
20. G. V. Dunne, Eur. Phys. J. Spec. Top. **223**, 1055 (2014).
21. G. Mourou, T. Tajima, and S. V. Bulanov, Rev. Mod. Phys. **78**, 309 (2006).
22. A. di Piazza, C. Müller, K. Z. Hatsagortsyan, and C. H. Keitel, Rev. Mod. Phys. **84**, 1177 (2012).
23. N. B. Narozhny and A. M. Fedotov, Eur. Phys. J. Spec. Top. **223**, 1083 (2014).
24. A. Ringwald, Phys. Lett. B **510**, 107 (2001).
25. R. Alkofer, M. B. Hecht, C. D. Roberts, et al., Phys. Rev. Lett. **87**, 193902 (2001).
26. N. B. Narozhny and A. M. Fedotov, Contemp. Phys. **56**, 249 (2015).
27. B. M. Karnakov, V. D. Mur, S. V. Popruzhenko, and V. S. Popov, Phys. Usp. **58**, 3 (2015).
28. V. S. Popov, JETP Lett. **13**, 185 (1971).
29. V. S. Popov, Sov. Phys. JETP **34**, 709 (1971).
30. V. S. Popov, Phys. Usp. **43**, 211 (2000).
31. V. S. Popov, Phys. Usp. **47**, 855 (2004).
32. V. S. Popov, JETP Lett. **74**, 133 (2001); V. S. Popov, J. Exp. Theor. Phys. **94**, 1057 (2002).
33. V. S. Popov, Phys. Lett. A **218**, 83 (2002); in *I. Ya. Pomeranchuk and Physics at the Turn of Centuries* (World Scientific, Singapore, 2003), p. 496.
34. L. V. Keldysh, Sov. Phys. JETP **20**, 1307 (1964).
35. *Special Issue on 50 Years of Optical Tunneling*, J. Phys. B **47** (20) (2015).
36. A. M. Perelomov, V. S. Popov, and M. V. Terent'ev, Sov. Phys. JETP **23**, 924 (1966).
37. A. M. Perelomov, V. S. Popov, and M. V. Terent'ev, Sov. Phys. JETP **24**, 207 (1966).
38. V. S. Popov, V. P. Kuznetsov, and A. M. Perelomov, Sov. Phys. JETP **26**, 222 (1967).
39. L. D. Landau, Phys. Zs. Sowjet. **1**, 88 (1932).
40. L. D. Landau and E. M. Lifshitz, *Course of Theoretical Physics*, Vol. 3: *Quantum Mechanics: Non-Relativistic Theory* (Nauka, Moscow, 1989, 4th ed.; Pergamon, New York, 1977, 3rd ed.).
41. N. B. Narozhny, S. V. Bulanov, V. D. Mur, and V. S. Popov, Phys. Lett. A **330**, 1 (2004).
42. V. S. Popov, V. D. Mur, B. M. Karnakov, and S. G. Pozdnyakov, Phys. Lett. A **358**, 21 (2006).
43. V. S. Popov, Phys. At. Nucl. **68**, 686 (2005).
44. L. D. Landau and E. M. Lifshitz, *Course of Theoretical Physics*, Vol. 2: *The Classical Theory of Fields* (Pergamon, Oxford, 1975).
45. L. D. Landau and E. M. Lifshitz, *Course of Theoretical Physics*, Vol. 1: *Mechanics* (Nauka, Moscow, 1982; Pergamon Press, New York, 1988).
46. V. D. Mur, B. M. Karnakov, and V. S. Popov, J. Exp. Theor. Phys. **87**, 433 (1998).
47. B. M. Karnakov, V. D. Mur, and V. S. Popov, J. Exp. Theor. Phys. **105**, 292 (2007).
48. V. S. Popov, V. D. Mur, and B. M. Karnakov, JETP Lett. **66**, 229 (1997).
49. Yu. N. Demkov and G. F. Drukarev, Sov. Phys. JETP **20**, 614 (1964).
50. V. S. Popov, V. D. Mur, B. M. Karnakov, and S. G. Pozdnyakov, J. Exp. Theor. Phys. **102**, 760 (2006).
51. E. Brezin and C. Itzikson, Phys. Rev. D **2**, 1191 (1970).
52. L. V. Keldysh, private communication (2001).
53. E. Yahnke, F. Emde, and F. Lösch, *Tables of Higher Functions* (McGrawHill, New York, 1960, Nauka, Moscow, 1977).
54. N. B. Narozhny and A. I. Nikishov, Sov. J. Nucl. Phys. **11**, 596 (1970).
55. L. V. Keldysh, Sov. Phys. JETP **6**, 763 (1957).
56. W. Franz, Z. Naturwiss. **13a**, 484 (1958).
57. N. B. Narozhny and M. S. Fofanov, J. Exp. Theor. Phys. **90**, 415 (2000).
58. S. S. Bulanov, N. B. Narozhny, V. D. Mur, and V. S. Popov, J. Exp. Theor. Phys. **102**, 9 (2006).
59. S. S. Bulanov, V. D. Mur, N. B. Narozhny, et al., Phys. Rev. Lett. **104**, 220404 (2010).
60. V. S. Popov, Doctoral (Phys. Math.) Dissertation (Inst. Theor. Exp. Phys., Moscow, 1974).
61. C. Eckart, Phys. Rev. **35**, 1303 (1930).
62. V. S. Popov and A. M. Perelomov, Sov. Phys. JETP **29**, 738 (1969).

Translated by K. Shakhlevich